

On the global hydration kinetics of tricalcium silicate cement

F. Tzschichholz^{1,2} and H. Zanni²

¹ *Department of Physics, Norwegian University of Science and Technology,
N-7034 Trondheim, Norway*

² *Laboratoire de Physique et Mécanique des Milieux Hétérogènes (CNRS, URA 857),
École Supérieure de Physique et de Chimie Industrielle de la Ville de Paris,
10 rue Vauquelin, 75231 Paris Cedex 05, France*

(June 24, 2021)

We reconsider a number of measurements for the overall hydration kinetics of tricalcium silicate pastes having an initial water to cement weight ratio close to 0.5. We find that the time dependent ratio of hydrated and unhydrated silica mole numbers can be well characterized by two power-laws in time, $x/(1-x) \sim (t/t_x)^\psi$. For early times $t < t_x$ we find an ‘accelerated’ hydration ($\psi = 5/2$) and for later times $t > t_x$ a ‘deaccelerated’ behavior ($\psi = 1/2$). The crossover time is estimated as $t_x \approx 16$ hours. We interpret these results in terms of a global second order rate equation indicating that (a) hydrates catalyse the hydration process for $t < t_x$, (b) they inhibit further hydration for $t > t_x$ and (c) the value of the associated second order rate constant is of magnitude $6 \cdot 10^{-7} - 7 \cdot 10^{-6}$ liter mol⁻¹ s⁻¹. We argue, by considering the hydration process actually being furnished as a diffusion limited precipitation that the exponents $\psi = 5/2$ and $\psi = 1/2$ directly indicate a preferentially ‘plate’ like hydrate microstructure. This is essentially in agreement with experimental observations of cellular hydrate microstructures for this class of materials.

PACS number(s):81.30.Mh, 61.43.-j, 81.35.+k

I. INTRODUCTION

Heterogeneous solid-state transformations are of great importance and practical interest in industrial and technological applications. Perhaps most prominent examples are transformations within alloys and steels playing a so crucial role for their mechanical and durability properties. Solid-state transformations are frequently accompanied by microstructural changes within the material in form of precipitating (segregating) phases from (solid) solutions. In its simplest form the transformation takes place between a major component acting as a solvent and an initially solvated phase. The precipitation process of the solvated phase is usually considered to happen in three main stages; phase nucleation, phase growth, and finally a coarsening process leading to a homogenisation of microstructural geometrical properties [1,2]. Further below we will employ basic concepts of solid-state transformation in order to interpret the experimentally observed hydration kinetics of cement, See Section III.

The massive introduction of hydraulic binders into daily engineering problems challenges a better understanding on how these materials work. Beside this are cementing processes also of great importance for certain geological problems, i.e., for the formation, properties and behaviour of sedimentary basins [3]. Typical hydraulic binders are plaster, cement, mortar, and concrete. In the following we will focus on the hydration of neat Portland cement (tricalcium silicate) more closely.

Basic phenomenological aspects of cement hydration can be characterized as follows. Initially fine grained cement powder (here tricalcium silicate, $C_3S \equiv Ca_3SiO_5$, with grain diameters typically ranging between $5 \mu m$ and $50 \mu m$ [4]) is mixed well with water. Tricalcium silicate is a well crystallized compound ($\rho = 3.21 g cm^{-3}$) and the employed pow-

ders typically have specific surface areas of order of $3 \cdot 10^3 cm^2 g^{-1}$ [5]. Rapidly after mixing the cement particles start to dissolve. The principal reaction products are solvated ions (Ca^{2+} , OH^- and $H_2SiO_4^{2-}$) diffusing within the solvent. The ion concentrations are bounded themselves by finite solubility products above which hydrate phases start to precipitate from solution, preferable on surfaces of already existing hydrates. There are two associated hydrates, a) the cement hydrate ($C_{1.5}SH_{2.5} \equiv (CaO)_{1.5}(SiO_2)(H_2O)_{2.5}$) and b) the Portlandite ($CH \equiv Ca(OH)_2$), which compete for the common calcium and hydroxyl ions. The cement hydrate ($\rho = 2.35 g cm^{-3}$) is amorphous in contrast to the crystalline Portlandite ($\rho = 2.24 g cm^{-3}$).

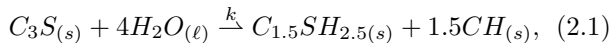
The process of cement dissolution, ion diffusion, and hydrate precipitation is usually referred as ‘cement hydration’. The ion diffusion represents the physical coupling between the chemical dissolution and precipitation reactions leading to a complex physico-chemical evolution of hydrate microstructure.

In Fig. 1 we show a hydrated microstructure after 40 hours of hydration time. Typical is the leaf/foil-like structure.

In the following we shall propose on the basis of already published NMR measurements an empirical global reaction rate law for the hydration of cement pastes for initial water to cement weight ratios $w/c = 0.5$. The observed values for the kinetics exponents can be understood – in parts – by classical solid-state transformation theory.

II. EXPERIMENTAL RESULTS AND KINETIC RELATIONSHIPS

The hydration of cement is spontaneous (exothermic) and irreversible and can be characterized by the global net reaction [5,6],



where k denotes an effective rate constant characterizing the solid to solid conversion rate. Because Eq. (2.1) describes a net reaction originating from various subprocesses the stoichiometric numbers in Eq. (2.1) are *not* related to the kinetic exponents of the overall reaction rate law. The kinetics of cement hydration has been experimentally studied to some extent by calorimetric and conductimetric measurements [5,7], by X-ray diffraction [8,9], by Raman spectroscopy [10], as well as by NMR spectroscopy [11–14].

A. NMR Measurements

^{29}Si NMR spectroscopy has been used to experimentally determine the CSH growth rate [11–14]. The employed method (Single Pulse Excitation with Magic Angle Spinning (MAS/SPE)) is based on the fact that in the NMR spectrum the signal of the C_3S silicon nuclei (monomer) is separated from those of CSH silicon nuclei (dimers and trimers) [15]. The distinction of dimer (silicon chain ends) and trimer (inside silicon chains) signals has been used to investigate the polymerization process within the cement hydrate, see for example Ref. 12.

In order to enhance the signal/noise ratio one generally needs to accumulate a great number of times the NMR signal. To achieve these accumulations and in order to obtain quantitative information about the populations of the different chemical species present in the specimen, one needs to strictly respect the relaxation of each population between subsequent accumulations. We have selected from the literature results obtained taking this condition into account [11–13]. NMR signal intensities, I_k , are in general proportional to the absolute number n_k of excited silicon nuclei of species k within the sample, $I_k = \Gamma n_k$, with Γ being the constant of the measurement (species k denotes a silicon nuclei belonging to a monomer, dimer, or trimer silicon cluster). The proportionality constant is usually eliminated by considering relative signal intensities $I_k / \sum_j I_j$ which correspond to mole fractions $x_k = n_k / \sum_j n_j$. The constant $\sum_j n_j$ defines the absolute silicon mass scale. The NMR measurements we refer to, provide plots of the time-dependent mole fractions for monomer, dimer and trimer silicon nuclei [11–13]. However, plots for mole fractions show, as will be demonstrated below, more complex algebraic behavior.

B. Schematic Representation

In order to get an idea about the global hydration kinetics of cement we consider the chemical *net* reaction (2.1) in a more schematic representation,



where the species A and B refer to silica nuclei of C_3S and CSH respectively. We denote the anhydrous C_3S (monomer) mole fraction as $x_A(t)$ and the CSH

(dimer as well as trimer) mole fraction as $x_B(t)$, i.e., $x_A(t) + x_B(t) = 1$.

The reader is reminded that Eq. (2.2) describes precisely a solid–state transformation as mentioned in the introduction, however, there is one fundamental difference in that the dimeric and trimeric silicon nuclei B are not *initially solvated* within the silicon monomers A . The B nuclei become rather formed within the liquid solution which does not appear in Eq. (2.2).

It is here the place to say something about the range of validity, the similarities, and the differences of Eqs. (2.1) and (2.2).

Strictly speaking, the above net reactions can only hold, if the employed water to cement weight ratio is not too high, that is to say the number of solvated ions should be always orders of magnitudes lower than the number of molecules belonging to the solid state, i.e., Eqs. (2.1) and (2.2) are *inconsistent* in the limit of infinite dilution. A proximate condition for this is a comparison of the cement to water concentration with the solubility of Portlandite, S_{CH} , $n_{C_3S}(t_0)/V_{H_2O}(t_0) \gg S_{CH} \approx 2 \cdot 10^{-2} \text{ mol liter}^{-1}$, or $w/c \ll 200$. The here considered experimental data certainly fulfill this condition, i.e., $w/c \approx 0.5$.

Furthermore Eq. (2.1) describes a solid–liquid to solid transformation, however, Eq. (2.2) a solid to solid transformation. It is thus natural that both reactions describe very different things, if the initial water to cement ratio is so low that the water severely becomes a limiting reactant for the hydration process (case of very thick pastes). To be more specific, the hydration following Eq. (2.1) cannot be completed for *chemical* reasons, if $4n_{C_3S}(t_0) > n_{H_2O}(t_0)$ or equivalently if $w/c < (w/c)^* = 0.31$. It is, a priori, difficult to judge whether the employed experimental water/cement ratio $w/c = 0.5$ is sufficiently large in order to exclude a systematic effect on hydration due to limiting water. However, as we will see further below, considering the kinetics of the ‘deacceleration’ period, water is very unlikely a chemically limiting reactant. It is, however, not possible to determine from the considered measurements any water-specific kinetic exponent for the associated rate law of Eq. (2.1). The determination of such a dependency, would require a set of experiments, conducted for different initial water to cement ratios. Similarly it is not possible to determine kinetic exponents for Portlandite (CH) from the considered measurements, because n_{CSH} is directly proportional to n_{CH} at every instant. In order to isolate the kinetic influence of precipitated Portlandite on the overall hydration kinetics one needs to break up the direct proportionality between n_{CSH} and n_{CH} . Preferable this could be done by examination of the hydration rate dependence for different initial CH admixtures, i.e., $n_{CH}(t_0) > 0$. Bearing the foregoing caveats in mind, it should be obvious why we consider the schematic reaction (2.2). We are only in position to characterize the kinetic influence of reactants and products on the cement hydration. But already this limited information will be, in our opinion, informative.

C. Kinetic Relationships

In the following we consider the ratio of silica mole fractions,

$$f(t) = x_B(t)/x_A(t), \quad (2.3)$$

varying between 0 (no hydrates at time $t = 0$) and ∞ (complete hydration at time $t = \infty$). Figure 2 shows a double-logarithmic plot of $f(t)$ versus the hydration time. This figure reveals several interesting facts about the hydration kinetics which will be addressed in this paper. We note that the considered experimental data have been taken from three independent publications obeying similar experimental conditions (room temperature, normal pressure, geometry of specimens, and initial water/cement weight ratio $w/c = 0.5$), see [11–13] for details. The relatively narrow scatter of the data over order of magnitudes demonstrates consistent and reproducible measurements.

We observe, within in the scatter, two power laws separated by a sharply defined characteristic time $t_\times = 16 \text{ hours}$ with value $f_\times \equiv f(t_\times) = 0.6$. For the ‘early’ hydration period ($t < t_\times$) we obtain,

$$f(t) = f_\times \left(\frac{t}{t_\times}\right)^\gamma, \quad (2.4)$$

with an exponent $\gamma = 2.5$. Below 5 hours of hydration time there are no quantitative NMR data available, because of the bad signal/noise ratio for the *CSH*. Above $t_\times = 16 \text{ hours}$ the hydration dramatically slows down,

$$f(t) = f_\times \left(\frac{t}{t_\times}\right)^\delta, \quad (2.5)$$

with $\delta = 0.5$. This second period takes place from 16 hours to at least $8 \cdot 10^3 \text{ hours}$ of hydration time. Equations (2.4) and (2.5) define a continuous dependency in time. However, the first derivative of $f(t)$ taken at t_\times is not continuous, which might appear unphysical. The discontinuity in df/dt arises, because we have assumed a zero crossover range in Eqs. (2.4) and (2.5) to obtain the best representation of experimental data. It is interesting to note, that an ansatz of the form

$$t/t_\times = 2^{-1/m}[(f/f_\times)^{\alpha m} + (f/f_\times)^{\beta m}]^{1/m}, \quad (2.6)$$

with proper chosen exponents $\alpha = 0.4$ and $\beta = 2.0$ gives a quite satisfactory representation of data for high integers of m , see Fig. 2 [16]. The best representation is found for $m \rightarrow \infty$, which corresponds to Eqs. (2.4) and (2.5).

In the following we propose relations between the above mentioned exponents γ and δ and the kinetic exponents of an overall rate equation. The observed exponents will allow for some general statements about the hydration mechanisms.

We note, that from Eq. (2.3) the trivial relations

$$x_A(t) = \frac{n_A(t)}{n_A(t_0)} = \frac{1}{1+f(t)}, \quad (2.7)$$

and

$$x_B(t) = \frac{n_B(t)}{n_A(t_0)} = \frac{f(t)}{1+f(t)}, \quad (2.8)$$

follow, where $n_A(t_0)$ characterizes the absolute silica mass scale. The overall rate equation for x_A and x_B has to be first order in time,

$$-\frac{d}{dt}x_A = \frac{d}{dt}x_B = \frac{1}{(1+f)^2} \frac{d}{dt}f. \quad (2.9)$$

One particular observation from Eqs. (2.7), (2.8), and (2.9) is that the global hydration rate can be represented as a product of powers of the mole fractions x_A and x_B , if $\frac{d}{dt}f$ follows a power-law in f . In such case the reaction is of overall order two and $f(t)$ follows a power-law in time, except for $\frac{d}{dt}f \sim f$ which yields an exponential dependency in time. We have already mentioned, considering the experimental results in Fig. 2, that $f(t)$ follows indeed two power-laws, Eqs. (2.4) and (2.5), separated by a characteristic time t_\times . Thus it is possible to extract two rate laws from the measurements; one for ‘early’ times $t < t_\times$ and another one for ‘late’ times $t > t_\times$. Consider $f(t) = f_\times \cdot (t/t_\times)^\psi$ where for times $t < t_\times$, $\psi = \gamma$ and for times $t > t_\times$, $\psi = \delta$, according to Eqs. (2.4) and (2.5). The associated first order differential equation is $(d/dt)f = \psi t_\times^{-1} f_\times^{1/\psi} f^{(\psi-1)/\psi}$. Inserting this into Eq. (2.9) and resorting with respect to factors x_B and x_A [Eqs. (2.8) and (2.7)] we obtain the explicit rate equation in terms of mole fractions,

$$-\frac{d}{dt}x_A = \frac{d}{dt}x_B = \psi t_\times^{-1} f_\times^{1/\psi} x_B^{\frac{\psi-1}{\psi}} x_A^{\frac{\psi+1}{\psi}}, \quad (2.10)$$

with $\psi = 2.5$ for $t < t_\times$ and $\psi = 0.5$ for $t > t_\times$.

Furthermore, by passing from mole fractions to concentrations, it is possible to determine the approximate effective rate constant(s) from the experimentally observed crossover point, the extracted exponents, and the initial water to cement weight ratio. It is convenient to consider first the initial concentration $[A]|_{t_0} = n_A(t_0)/V_0$ of cement in the overall specimen volume $V_0 = V_{C_3S}(t_0) + V_{H_2O}(t_0)$ [17],

$$\frac{1}{[A]|_{t_0}} = \left(1 + \frac{\rho_{C_3S}}{\rho_{H_2O}} \cdot \frac{w}{c}\right) v_{C_3S} \approx 0.18 \text{ liter mol}^{-1}, \quad (2.11)$$

with $\rho_{C_3S}/\rho_{H_2O} = 3.21$ and $v_{C_3S} = 7.2 \cdot 10^{-2} \text{ liter mol}^{-1}$ being the relative density and the molecular volume of cement respectively. The considered water to cement weight ratio is $w/c = 0.5$.

We find for the ‘accelerated’ period ($t < t_\times$),

$$-\frac{d}{dt}[A] = \frac{d}{dt}[B] = k_{t < t_\times} \cdot [B]^{0.6}[A]^{1.4}, \quad (2.12)$$

with $k_{t < t_\times} = 2.5[A]|_{t_0}^{-1} t_\times^{-1} f_\times^{0.4} \approx 7 \cdot 10^{-6} \text{ liter mol}^{-1} \text{ s}^{-1}$, and for the ‘deaccelerated’ period ($t > t_\times$)

$$-\frac{d}{dt}[A] = \frac{d}{dt}[B] = k_{t > t_\times} \cdot [B]^{-1.0}[A]^{3.0}, \quad (2.13)$$

with $k_{t > t_\times} = 0.5[A]|_{t_0}^{-1} t_\times^{-1} f_\times^{2.0} \approx 6 \cdot 10^{-7} \text{ liter mol}^{-1} \text{ s}^{-1}$.

III. INTERPRETATION

Before we are going to present a possible explanation for the hydration kinetics as manifested in Eqs. (2.12) and (2.13) we would like to give a brief account on another representation of the hydration kinetics being more widespread in cement literature, i.e., the degree of hydration $\alpha(t)$. The degree of hydration is usually referred as the relative amount (mole fraction) of hydrated cement [18], $\alpha(t) \equiv x_B(t) = 1 - x_A(t)$. Therefore Eq. (2.8) gives the relationship between $\alpha(t)$ and $f(t)$ as defined in Eq. (2.3). Typical experimental curves for the degree of hydration exhibit sigmoidal shapes in linear representations. The observed inflection points, however, do in general not possess any particular significance for a change in chemical mechanism. This can be seen for example by assuming in Eq. (2.10) $\Psi > 1$ for *all times*. The degree of hydration will show an inflection point though there is only a single chemical mechanism (rate law) operative. Therefore it is not reliable to read off characteristic times from $\alpha(t)$ diagrams. While $\alpha(t)$ approximates $f(t)$ well if $f \ll 1$ (early hydration) the discrepancy becomes very large for $f \gg 1$ (late hydration).

The foregoing remark has hopefully illustrated why we have avoided degree of hydration diagrams in our considerations. As another motivation for our approach we present in Fig. 3 a so-called ‘Avrami-Plot’ for the hydrated silica amount, i.e., a test on the stretched exponential relationship $x_B = 1 - \exp(-(t/\tau)^k)$. Such empirical relationships are frequently found for overall transformations [1]. It can be clearly seen from Fig. 3 that the hydration data *cannot* be described by such a relation.

The kinetic equations Eqs. (2.12) and (2.13) allow to make somewhat more substantial statements about the global cement hydration mechanism(s). During the acceleration period already existing hydrates *catalyse* the precipitation of new hydrates (positive kinetic exponent for the products in Eq. (2.12)). The growth of *connected* hydrate structures appears thus to be thermodynamically more favorable than an uncorrelated ‘through solution’ precipitation mechanism.

On the other hand in the deceleration period ($t > t_x$) the ‘hydrate layers’ surrounding the cement grains increasingly separate reacting anhydrous cement and water and thus hinder/block further C_3S dissolution. The hydrates are acting in the decelerated period as *inhibitors* (negative exponent for the products in Eq. (2.13)). The inverted role of hydration products during the accelerated and decelerated periods appears to be experimentally evident from the foregoing considerations.

A widespread assertion in cement literature is that ‘early’ hydration is controlled by chemical kinetics whilst ‘late’ stage kinetics is being diffusion controlled. We agree with the later assumption that ion diffusion most probably represents the rate controlling step within the deceleration period. This is in fact strongly indicated by the very low hydration rate at large times, see Fig. 2.

However, there is no direct indication that the ac-

celeration kinetics is chemically limited. Obviously Eq. (2.12) *cannot* describe initial nucleation (approximately within the first 15 *min*) because there exist no products at this times at all ($[B]|_{t_0} = 0$). On the other hand the early nucleation period is not accessible employing the here considered experimental techniques, so there is no conflict in interpretation. One just has to keep in mind that all experimental data points as well as the thereof extracted power-laws are beyond the nucleation period.

After the first few minutes of bringing cement and water into contact, the ions in solution rise their concentrations far beyond the equilibrium solubilities, without precipitating at all. This can be understood by viewing the process of heterogeneous nucleation as overcoming a thermodynamical barrier (supersolubility [7]). Being supersaturated the hydrate nucleation happens on the cement grain surfaces [19,18]. At this instant a more or less significant part of the solution is strongly oversaturated with respect to the equilibrium solubility. The further precipitation (growth) of the hydrates can thus be regarded to happen approximately within a spatial uniform oversaturated solution (oversaturated interface layer). This is in so far of concern as the uniformity of ‘initial conditions’ is crucial to predict kinetic exponents for diffusion controlled reactions. It also supposes that the nucleation rate tends rapidly to zero as the hydrate microstructure further develops.

The hydrate microstructure has been experimentally classified for a water to cement ratio $w/c = 0.47$. Within the first 4 *hours* foil-like microstructure precipitation is reported to happen radially away from the cement grains (typical dimensions $< 0.5 \mu\text{m}$ and $x_B < 10^{-2}$). Thereafter ($< 24 \text{ hours}$) the formation of a gelatinous layer surrounding the cement grains have been observed (thickness $\approx 0.5 \mu\text{m}$ and $x_B(24 \text{ h}) \approx 0.3$). Also needle-like precipitates have been found. Finally after several days crumpled interlocking foils are observed (comp. Fig. 1). It has been also reported that the precipitated microstructure morphologies are strongly influenced by the available interparticle spacings [19]. There is presently no straightforward way to predict/calculate microstructural morphologies for such complex systems, however, recently developed heterogeneous reaction-diffusion models have received considerable interest in this context [20].

The growth of a precipitate is kinematically very complex. The precipitated geometry (microstructure) cannot be predescribed in general beyond the initial conditions but is rather a *result* of the associated interface dynamics. The most simplest case is governed by the growth of spherical precipitates of radius R from an initially supersaturated solution of concentration \bar{c} . Let $c = c(r)$ denote the particle concentration in the solvent, $c_{s\ell}$ the particle concentration within the precipitate at the interface, $c_{\ell s}(R)$ the particle concentration within the solvent at the interface and D the diffusion coefficient of particles in the solvent. One has from continuity of mass,

$$\frac{dR}{dt} = \frac{D}{c_{s\ell} - c_{\ell s}(R)} \cdot \left(\frac{dc}{dr} \right)_{r=R} \quad (3.1)$$

This is the equation of motion for the interface (in spherical co-ordinates). It establishes the direct proportionality between *local* growth rate and particle current density at the interface. In general $c_{\ell s}$ depends, as a consequence of interfacial tension, on the (local) interface curvature. If the precipitate is not too small one often assumes the zero curvature limit, i.e., $c_{\ell s}(R) \approx c_{\ell s}(\infty)$. The most interesting point in Eq. (3.1) is that the gradient of c contains ‘global information’ about the interface because $c(r)$ is the solution of the (stationary) diffusion equation,

$$\Delta c(r) = 0, \quad (3.2)$$

obtained under boundary conditions $c(\infty) = \bar{c}$ and $c(R) = c_{\ell s}(\infty)$. The solution of Eqs. (3.1) and (3.2) is the well known parabolic growth law [1],

$$R^2 - R_0^2 = 2D \frac{\bar{c} - c_{\ell s}(\infty)}{c_{s\ell} - c_{\ell s}(\infty)} (t - t_0). \quad (3.3)$$

Similarly a parabolic solution is also obtained for the growth of a flat interface. More generally does the local growth rate dynamically depend on (at least) two competitive mechanisms (a) flattening of high curvature regions due to interfacial tension and (b) sharpening of these regions due to preferential diffusive growth at these ‘tips’. Numerical boundary integral methods have been developed in order to study the associated interface dynamics and instability, e. g. see Ref. [21]. For a perturbative treatment see for example Ref. [22].

Despite the complexity of involved microstructural transformations the natural question arises whether there exists at a given time a *typical microstructure* and a *typical mode of growth* within the system.

Suppose the case of a vanishing nucleation rate during precipitate growth. If the precipitating structure grows geometrically in form of a plate (see the above experimental classification scheme) then the variation in mole fraction of precipitated phase in time is predicted theoretically for $x_B \ll 1$ as $x_B \sim (t/\tau)^{5/2}$ [1] with τ being a characteristic timescale for the growth [23]. The plate’s rim grows at a constant rate while its thickness grows parabolically in time, explaining the exponent $5/2$. For $x_B \ll 1$ one can replace the quantity $f(t)$ by $x_B(t)$ in all foregoing considerations. One is lead to the conclusion that for early foil-like hydrate growth $\gamma = 5/2$ and $(\psi - 1)/\psi = 3/5$ in Eqs. (2.4) and (2.10) respectively. This is in agreement with the considered measurements, see Fig. 2.

What causes the observed slowing down of the hydration process? If a single foil would precipitate in a spatially infinite supersaturated solution there would be no obvious reason for a slowing down of the hydration process as there exists no characteristic length scale. However, the here considered case of cement paste is an assembly of small anhydrous cement grains immersed in water. The mean free distance between particles has to be considered as a typical length scale for the transport and for the precipitation process ($x_B \ll 1$). The size of the growing flakes *cannot* exceed this because of spatial hindrance. Hence there must exist a typical time scale t_x at which the flakes change their mode of growth into thickening only. We interpret this typical time as the crossover

time $t_x \approx 16$ hours observed in Fig. 2. Growth of flakes in the thickening only mode is expected to happen parabolically in time for diffusion limited precipitation reactions [1]. Therefore we predict the exponents of the decelerated period to be $\delta = 1/2$ and $(\psi - 1)/\psi = -1$ in Eqs. (2.5) and (2.10) respectively, in agreement with the experimental data Fig. 2.

Apparently with the above assessments we have related the experimentally observed kinetic exponents of the hydration products to microstructural information. Certainly there is no unique mapping between kinetics and geometry, but this constitutes a complex question in terms of Eqs. (3.1) and (3.2) to be studied in future on its own right.

So far we have restricted our considerations to the case of a water to cement weight ratio $w/c = 0.5$. The question arises whether the kinetic exponents are universal and how the observed typical crossover quantities t_x and f_x do depend on w/c . We show in Fig. 4 experimental (replotted) data for three different w/c ratios. The data do not collapse, which is not so surprising because the typical interparticle spacing does depend on w/c . Qualitatively higher w/c ratios correspond to lower characteristic times t_x and lower hydrate ‘amounts’ f_x . For early times we observe kinetic exponents that do (apparently) depend on w/c . Interestingly are the kinetic exponents δ for the deceleration period in all cases close to $1/2$. However, we have not studied this in further detail because there are less experimental data available than for the standard case $w/c = 0.5$, i.e., the hydration curves need to be experimentally reproducible for given w/c .

IV. CONCLUSION

We have reconsidered NMR measurements on the overall hydration kinetics of tricalcium silicate pastes ($w/c = 0.5$) In Sec. IIB we briefly discussed the conditions for w/c to be fulfilled in order to allow a meaningful discussion in terms of a global net reaction and its schematic counterpart. In Sec. IIC we demonstrated that the time dependent ratio of hydrated and unhydrated silica mole numbers can be well characterized by two power-laws in time, $x/(1 - x) \sim (t/t_x)^\psi$. For early times $t < t_x$ we found an ‘accelerated’ hydration ($\psi = 5/2$) and for later times $t > t_x$ a ‘decelerated’ behavior ($\psi = 1/2$). The crossover time has been estimated as $t_x \approx 16$ hours. We interpreted these results in terms of a global second order rate equation indicating that (a) hydrates do catalyse the hydration process for $t < t_x$, (b) they do inhibit hydration for $t > t_x$ and (c) the value of the associated second order rate constant is of magnitude $6 \cdot 10^{-7} - 7 \cdot 10^{-6}$ liter mol⁻¹ s⁻¹. We have argued in Sec. III, by considering the hydration process actually being furnished as a diffusion limited precipitation that the exponents $\psi = 5/2$ and $\psi = 1/2$ directly indicate a preferentially ‘leaf’ like hydrate microstructure. This argument was supported by experimental observations of cellular hydrate microstructures for this class of materials.

ACKNOWLEDGMENTS

F. T. would like to acknowledge financial support from CEC under grant number ERBFMBICT 950009.

- [1] , V. Raghavan and M. Cohen in *Treatise on Solid State Chemistry, Vol. 5 Changes of State*, ed. by N.B. Hannay (Plenum Press, London, 1975) pp. 67–127.
- [2] G. Sauthoff, *J. de Physique IV* **6**, 87-97 (1996).
- [3] E.H. Oelkers and P.A. Bjorkum, *American Journal of Science* **296**, 420-52 (1996).
- [4] M.D. Cohen and R.D. Cohen, *J. Mat. Sci.* **23**, 3816-20, (1988).
- [5] P. Barret and D. Bertrandie, *Journal de Chimie Physique* **83**, 11/12, 765-75, (1986).
- [6] This is an approximation. A particularity of the cement hydration problem is that the appearing cement hydrate exhibits a variable stoichiometry in course of its formation ('solid solution'). The selected stoichiometries in Eq. (2.1) correspond to the 'late stage' proportions in cement hydration [5].
- [7] D. Damidot and A. Nonat, *Advances in Cement Research* **6** (21), 27-35, (1994).
- [8] S. Tsumura, *Zement Kalk Gips* **11**, 511-8 (1966).
- [9] I. Odler and H. Doerr, *Cement and Concrete Research* **9**, (2), 239-48 (1979).
- [10] M. Tarrida, M. Madon, B. Le Rolland and P. Colombat, *Advn. Cem. Bas. Mat.* **2**, 15-20 (1995).
- [11] C.M. Dobson, D.G.C. Goberdhan, J.D.F. Ramsay and S.A. Rodger, *J. Mat. Sci.* **23**, 4108-14 (1988).
- [12] A.R. Brough, C.M. Dobson, I.G. Richardson and G.W. Groves, *J. Mat. Sci.* **29**, 3926-40 (1994).
- [13] J. Hjorth, J. Skibsted and H.J. Jakobsen, *Cement and Concrete Research* **18**, 789-98 (1988).
- [14] S.U. Al-Dulaijan, G. Parry-Jones, A.-H. J. Al-Tayyib and A. I. Al-Mana, *J. Am. Ceram. Soc.* **73**, (3), 736-39 (1990); H. Justnes, I. Meland, O.J. Bjoergum and J. Krane, *Adv. Cem. Res.* **3**, (11), 111-16 (1990).
- [15] J.G. Engelhardt and D. Michel, *High-Resolution solid state NMR of silicates and zeolites* (J. Wiley Editions 1987).
- [16] Note that $f(t)$ cannot be expressed as the sum of two powers in time because $\gamma > \delta$, compare Eqs. (2.4) and (2.5). However, the time can be expressed as a sum of two powers of $f(t)$.
- [17] We assume here a constant and characteristic reference volume V_0 . This is an approximation in that the hydrating system Eq. (2.1) undergoes a chemical shrinkage in course of the hydration (nominal ≈ 10 Vol %, however, in practice less).
- [18] H.F.W. Taylor, *Cement Chemistry*, (Academic Press, London, 1990).
- [19] H. M. Jennings, B. J. Dalgleish and P. L. Pratt, *J. Am. Ceram. Soc.* **64**, (10), 567–72 (1981).
- [20] F. Tzschichholz, H. J. Herrmann and H. Zanni, *Phys. Rev. E* **53**, (3), 2629-37 (1996).
- [21] D. A. Kessler, J. Koplik and H. Levine, *Adv. Phys.* **37**, 255-336 (1988).
- [22] R. Lovett, P. Ortoleva and J. Ross, *J. Chem. Phys.* **69**, (3), 947 (1978).
- [23] The timescale τ arises from such quantities as initial oversaturation, diffusion coefficients, and water-hydrate interface properties.

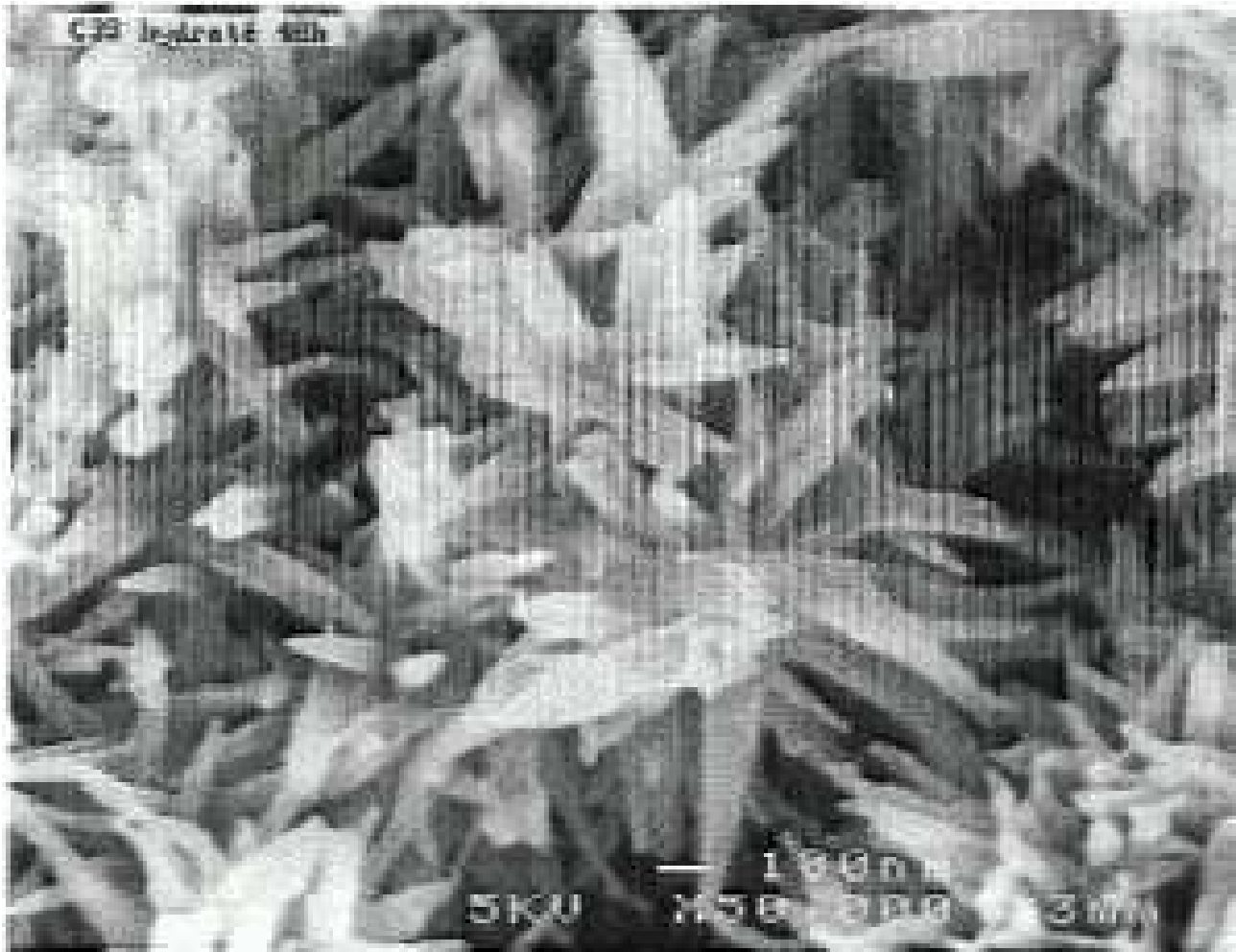


FIG. 1. SEM micrograph of hydrated tricalcium silicate cement after 40 hours hydration time. The initial water to cement ratio was 0.5. Note the leaf-like hydrate microstructure (with courtesy of Institute Francais du Petrole).

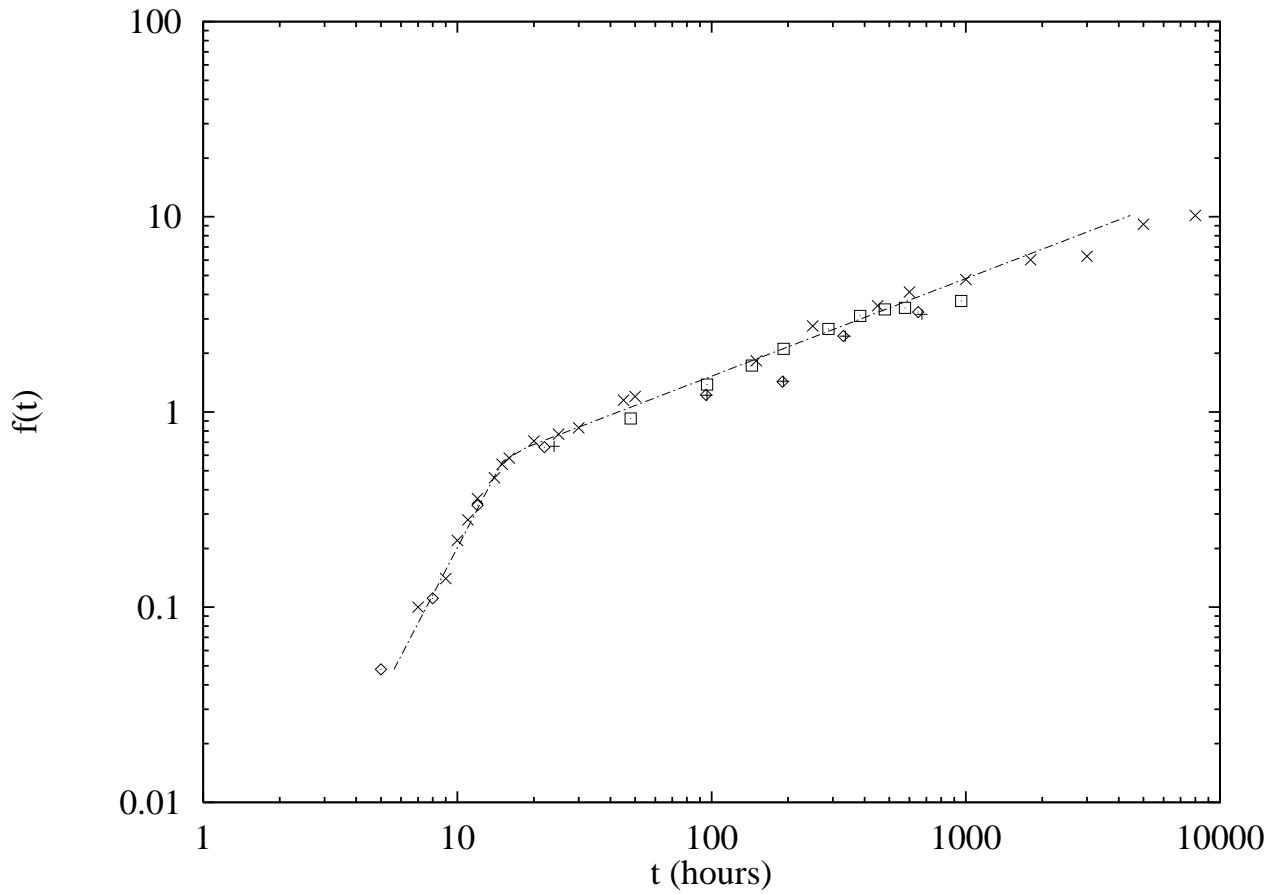


FIG. 2. Double logarithmic plot of the measured mole ratio between hydrated and unhydrated silica $f(t) = x_B/(1-x_B)$ as a function of hydration time t employing NMR and TGA (Thermogravimetry). All measurements correspond to a water to cement weight ratio $w/c = 0.5$ conducted under room temperature and normal pressure. The data are well represented by two power-laws: for $t < t_x$ by Eq. (2.4) ($\gamma = 2.5$) and for $t > t_x$ by Eq. (2.5) ($\delta = 0.5$). The dashed line shows the corresponding numerical fit according to Eq. (2.6) employing $t_x = 16$ hours, $f(t_x) = 0.6$, and $m = 20$. Data from (\diamond) Ref. 11 (NMR), (\times) Ref. 12 (NMR), (\square) Ref. 13 (NMR) and (+) Ref. 11 (TGA).

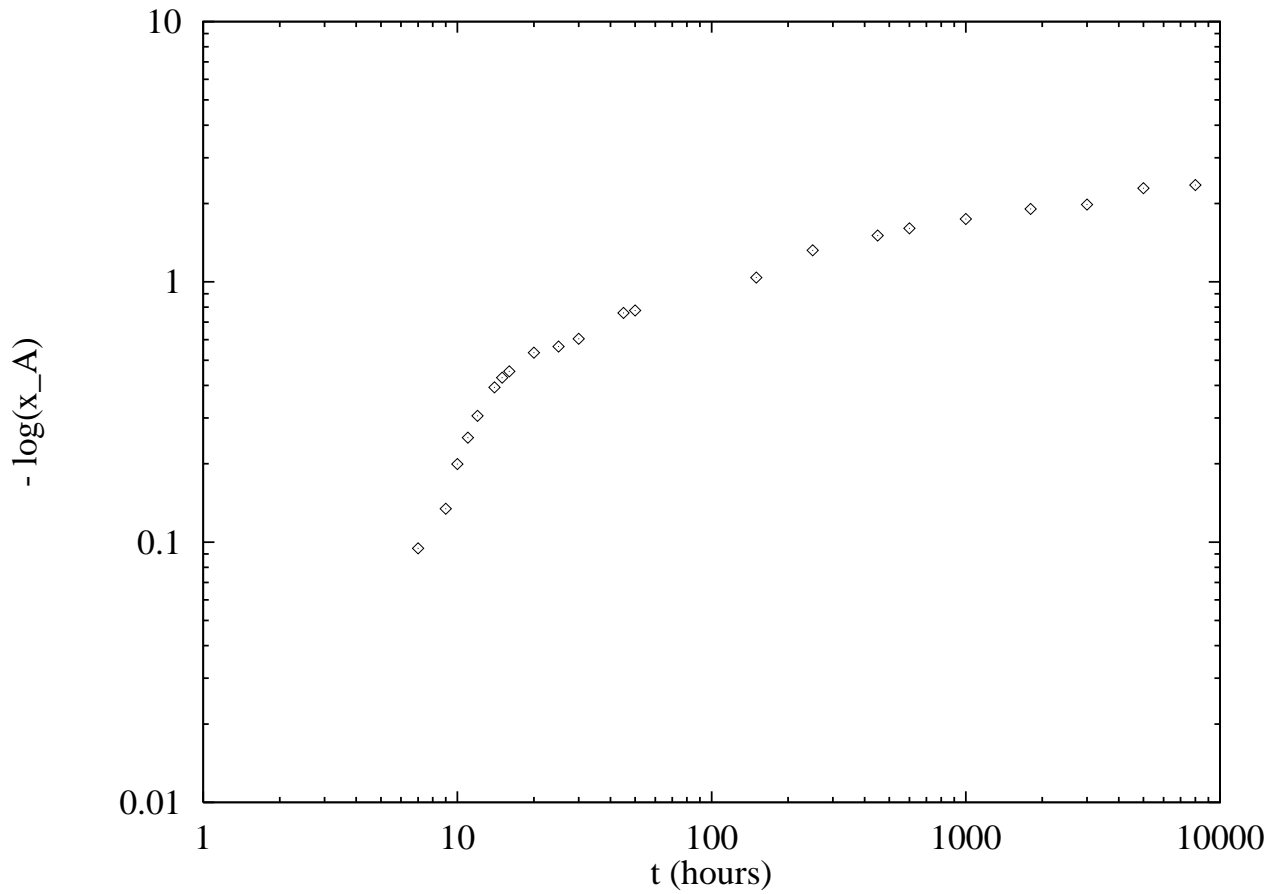


FIG. 3. ‘Avrami’-Plot for the amount of hydrated silica (double logarithmic plot of the negative logarithm of unhydrated silica amount $-\log(x_A)$ versus time t). If the hydration kinetics would follow a generalized Avrami–Johnson–Mehl law, i.e., $x_A = 1 - x_B = \exp(-(t/\tau)^k)$, the data should lay on a *single* straight line of slope k . It can be seen that this is *not* the case. The data were taken from Ref. 12 (NMR).

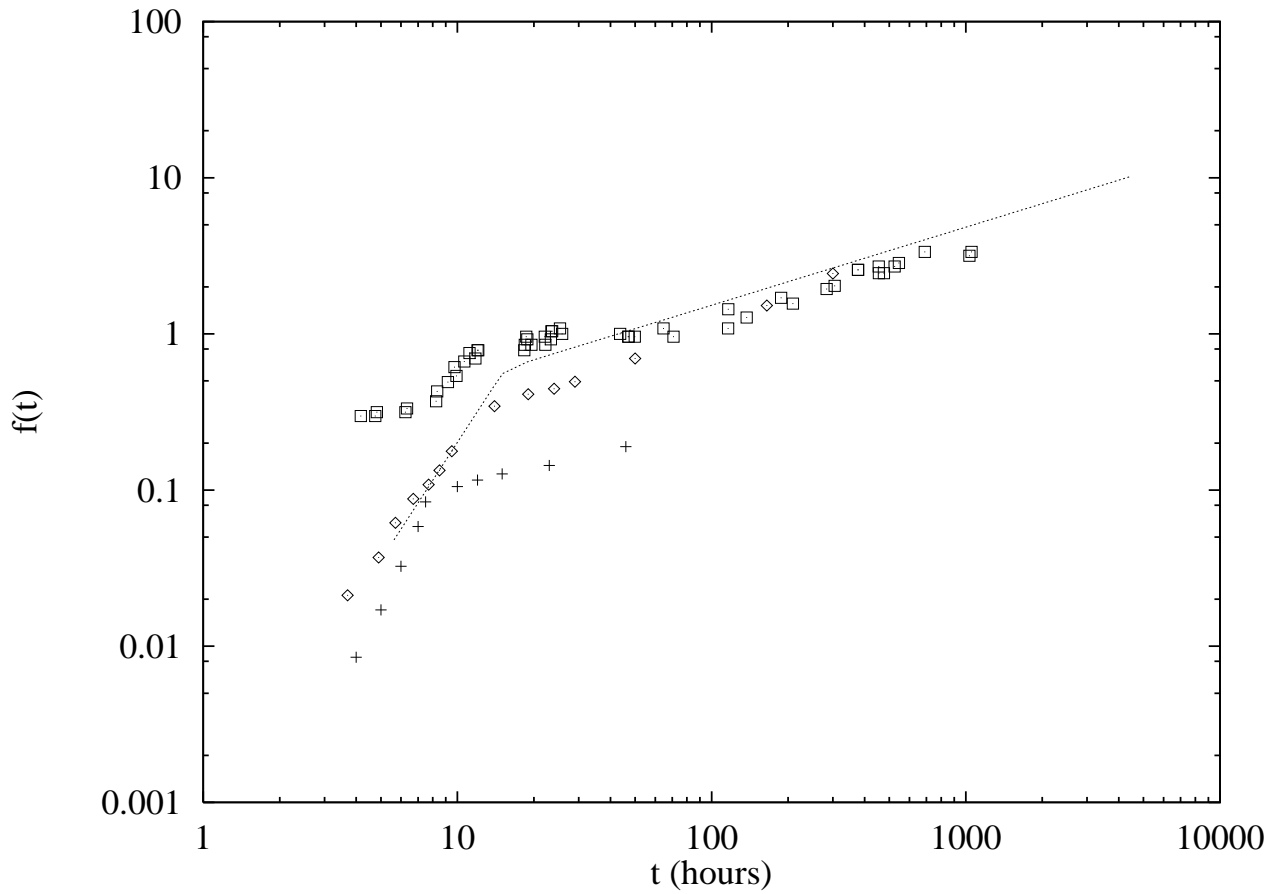


FIG. 4. Same representation as in Fig. 2 but for various water cement ratios employing XDR (x-ray diffraction) and Raman spectroscopy. The measurements were conducted at room temperature and normal pressure. The dashed line shows again the powerlaw fit corresponding to Fig. 2 for comparison purposes. Data from (\square) Ref. 10 (Raman, $w/c = 0.4$), (\diamond) Ref. 8 (XDR, $w/c = 0.45$) and ($+$) Ref. 9 (XDR, $w/c = 0.7$). Note that the data do not collapse, however, for large times they yield similar slopes $\approx 1/2$ compared to Fig. 2.